

Choroid plexus enlargement in acute neuroinflammation is tightly interrelated to the tyrosine receptor signalling

3 Felix Luessi^{†1}, Julia Schiffer^{†1}, Gabriel Gonzalez-Escamilla^{†1}, Vinzenz Fleischer¹, Sinah Engel¹,
4 Dumitru Ciolac¹, Thomas Koeck², Philipp S. Wild^{2,3,4,5}, Joel Gruchot⁶, Tobias Ruck⁶, Ahmed Othmann⁷,
5 Stefan Bittner¹, Sven G. Meuth⁶, Frauke Zipp¹, Olaf Stüve^{8,9}, Sergiu Groppa^{1*}

6 Author affiliations:

⁷ ¹Department of Neurology, Focus Program Translational Neuroscience (FTN), Rhine-Main
⁸ Neuroscience Network (rmn²), University Medical Center of the Johannes Gutenberg University Mainz;
⁹ Mainz, Germany.

² Preventive Cardiology and Preventive Medicine, Department of Cardiology, University Medical Center of the Johannes Gutenberg University Mainz; Mainz, Germany.

12 ³Clinical Epidemiology and Systems Medicine, Center for Thrombosis and Hemostasis (CTH),
13 University Medical Center of the Johannes Gutenberg University Mainz; Mainz, Germany.

¹⁴German Center for Cardiovascular Research (DZHK), partner site Rhine-Main; Mainz, Germany.

15 ⁵Systems Medicine Group, Institute of Molecular Biology (IMB); Mainz, Germany.

¹⁶Department of Neurology, Heinrich Heine University; Düsseldorf, Germany.

17 ⁷Department of Neuroradiology, University Medical Center of the Johannes Gutenberg University
18 Mainz; Mainz, Germany.

19 ⁸Department of Neurology, Peter O'Donnell Brain, University of Texas Southwestern Medical Center;
20 Dallas, TX, U.S.A..

21 ⁹VA North Texas Health Care System; Dallas, TX, U.S.A..

22 [†]These authors contributed equally to this work.

23 *Corresponding author:

24 Univ.-Prof. Dr. Sergiu Groppa, MBA

25 Department of Neurology, Focus Program Translational Neuroscience (FTN), Rhine-Main
26 Neuroscience Network (rmn²), University Medical Center of the Johannes Gutenberg University Mainz,
27 Langenbeckstrasse 1, 55131 Mainz, Germany

28 Tel: +49-6131-17 2998; Fax: +49-6131-17 47 2998; email: segroppa@uni-mainz.de

29

30 **Abstract**

31 The choroid plexus (ChP) plays a crucial function in neuroinflammation of the central nervous system
32 and in the immune response of the brain during neurodegeneration. Recent studies described a massive
33 ChP enlargement in patients with multiple sclerosis (MS) and active disease courses, but also in several
34 other neuroinflammatory and neurodegenerative conditions. Nevertheless, the exact basis and
35 pathophysiology behind ChP hypertrophy remains unclear. This study was designed to evaluate the
36 association of cerebrospinal fluid (CSF) proteomic spectra with brain MRI-derived volumetric measures
37 of ChP in two independent cohorts of MS patients, and to translationally validate the related molecular
38 mechanisms in the transcriptomic analysis of the ChP properties in a mouse model of experimental
39 autoimmune encephalomyelitis (EAE). Our analysis revealed five enriched proteins (*NTRK2*, *ADAM23*,
40 *SCARB2*, *CPM*, *CNTN5*) significantly associated with the ChP volumes in both of the MS cohorts. These
41 proteins relate closely to mechanisms of cellular communication, function (e.g. transmembrane tyrosine
42 receptor signalling (RTK) and vascular endothelial growth) and pathways involved in the regulation of
43 cellular plasticity (e.g. neuron differentiation, axonal remodelling and myelin regulation) as depicted by
44 molecular function analysis and validation of the results in the transcriptome from ChP tissue specific
45 for EAE. This work provides conclusive new evidence for the role of ChP in the context of
46 neuroinflammation and neurodegeneration, demonstrating the intriguing relationships between ChP
47 enlargement, CSF dynamics, and the development of neuroinflammatory and neurodegenerative
48 diseases. Our results are encouraging for the development of new therapeutic avenues (i.e. targeting
49 RTK signalling).

50 **Keywords:** multiple sclerosis, CSF proteomics, choroid plexus, neuroinflammation

51 **One sentence summary:**

52 Tyrosine receptor signalling is tightly associated with choroid plexus enlargement and is key in CSF
53 dynamics during a neuroinflammatory attack in MS

54

55

56 INTRODUCTION

57 Multiple sclerosis (MS) stands as the most prevalent chronic neuroinflammatory disease, causing
58 progressive disability. Regarding the complex and dynamic pathogenesis of MS, a growing body of
59 evidence has posed the importance of communication between the central nervous system (CNS) and
60 peripheral immune factors. In this particular context, the choroid plexus (ChP) has garnered significant
61 attention as a crucial structure for the regulation and propagation of inflammation at the barrier between
62 blood and the brain's extracellular fluid or cerebrospinal fluid (CSF (1), acting as a nexus for immune
63 cell trafficking, blood-brain barrier (BBB) regulation, cytokine production, and antigen presentation (2,
64 3). Regulating the entry of inflammatory cells into the brain and the trafficking of immune cells from
65 brain tissue into the CSF, the ChP plays a crucial role in both maintaining neuroimmune homeostasis
66 and responding to inflammatory and neurodegenerative brain conditions.

67 The choroid plexus is thought to critically contribute to the development and progression of MS (3-5).
68 Recent studies found ChP enlargements in patients with MS as compared to healthy controls and
69 demonstrated an association with functional impairment and disease progression (6-8). A recent study
70 showed that a larger ChP in MS patients as compared to controls may serve as a surrogate marker for
71 tracking neuroinflammation dependent disease progression, as well as being a marker for therapeutic
72 responses (6). The latest work also highlights also the potential of ChP as a translational brain imaging
73 biomarker for the quantification of neuroinflammation in humans and mice.

74 In recent years, transcriptomic approaches have been established as powerful tools for unravelling
75 molecular pathways and mechanistic networks associated with disease initiation and progression in
76 various neuroinflammatory and neurodegenerative disorders. Moreover, CSF proteomics were shown
77 to have the potential to contribute to the development of diagnostic tests, prognostic markers, and
78 therapeutic targets for various neurological disorders. Changes in specific proteins or protein patterns
79 provide illustrative insights into disease mechanisms and might aid in early disease stages to dissect
80 ongoing pathological abnormalities. In MS, neurofilament light chains (NFL) analyses were specifically
81 linked to acute injuries during relapses, as well as to neurodegeneration and the extent of axonal damage
82 (9, 10). Moreover, a number of proteins related to inflammation in the CSF have been associated with
83 the duration and advancement of MS (11, 12). Building upon these insights, our study endeavors to
84 explore the association between MRI-derived volumetric measures of the choroid plexus (ChP) and CSF
85 proteins implicated in neurobiological processes and neurological disorders. We aim to elucidate the
86 significance of ChP-related neuroinflammation by integrating translational insights from transcriptomic
87 data obtained from the experimental autoimmune encephalomyelitis (EAE) mouse model. By
88 investigating the interplay between ChP volumetrics and CSF protein profiles, our research seeks to
89 contribute to a deeper understanding of neuroinflammatory mechanisms and potentially unveil novel
90 avenues for diagnosing and managing neurological disorders.

91 RESULTS

92 *Clinical characteristics*

93 In our study, MRI, clinical and CSF proteomic data from 69 RRMS patients (discovery cohort) and 30
94 RRMS patients (replication cohort) were included. All patients were included during a relapse period,
95 thus, depicting acute neuroinflammatory damage. There was no significant difference between the
96 discovery cohort and the replication cohort on the main clinical characteristics (EDSS, disease duration,
97 mean age at CSF sampling and MRI). The demographic and clinical data of the MS patients are
98 summarized in table 1 after separating the MS patients in the discovery cohort from the replication
99 cohort. The comparison of ChP volumes with total brain volume (TBV) normalization between the
100 discovery and replication cohorts showed no significant difference just as the comparison of ventricle
101 volume between both of the cohorts (Figure 1). However, both cohorts showed an increased ChP volume
102 in comparison to the healthy controls (HC) (ANOVA $F_{(131,2)}=7.98$, $p=0.0006$).

103 **Associations between ChP integrity and CSF proteins spectra**

104 In the discovery cohort, 25 of the 92 proteins analysed were significantly associated with ChP volume.
105 In the replication cohort, ChP enlargement was linked with 10 proteins, with five of the proteins being
106 identical to those identified in the discovery cohort (Figure 2A). The depicted proteins included
107 Neurotrophic Receptor Tyrosine Kinase 2 (NTRK2) (Table 2, discovery pFDR=0.013, replication
108 pFDR=0.048), Disintegrin and Metalloproteinase Domain containing Protein 23 (ADAM23) (Table 2,
109 discovery pFDR=0.019, replication pFDR=0.045), Scavenger Receptor class B, member 2 (SCARB2)
110 (Table 2, discovery pFDR=0.028, replication pFDR=0.05), Carboxypeptidase M (CPM) (Table 2,
111 discovery pFDR=0.027, replication pFDR=0.044), and Contactin-5 (CNTN5) (Table 2, discovery
112 pFDR=0.033, replication pFDR=0.041).

113 **Protein enriched network analysis**

114 The PPI network, depicted in Figure 2B and constructed from proteins associated with ChP volume,
115 demonstrated notable similarities in both the discovery cohort (enrichment pFDR = 0.0042) and the
116 replication cohort (pFDR = 0.046) in terms of the most enriched genes. The identified network displayed
117 enrichment in 22 overlapping pathways, of which four were related to molecular functions and 18 were
118 related to biological processes (Figure 2C). The enriched molecular function pathways were
119 mechanisms of cellular communication (i.e., vascular endothelial growth, transmembrane tyrosine
120 receptor activity, and signalling), as well as growth factor receptor activity. Regarding the biological
121 process, the significant enriched functional pathways were related to regulation of plasticity (i.e., axon
122 modifications and myelin regulation), as well as to neuronal regulation (i.e., neuron generation,
123 differentiation, and migration).

124 **EAE ChP proteomics analysis**

125 To corroborate the findings obtained from the CSF of MS patients, we conducted a comparative analysis
126 with the transcriptomic profile derived from the ChP tissue specific to EAE. The ChP samples extracted
127 from the mice evidenced the involvement of immune molecule activity (particularly cytokines) and
128 cellular communication (also involving receptor signalling activity and transmembrane receptors) as
129 molecular processes; and immune and inflammation related pathways (involving leukocytes and
130 lymphocytes) as biological processes (Figure 3A; upper panels). A detailed overview of the identified
131 proteins within these enriched pathways is provided in supplementary table 1. The significant
132 participation of tyrosine kinase proteins, particularly NTRK2, in influencing ChP volume within the
133 human cohort compelled us to prioritize investigations into tyrosine-related pathways. The targeted
134 search analyses using terms involving 'tyrosine' revealed five related pathways (Figure 3B) implicated
135 in signalling and activity of the tyrosine kinase protein. The analysis of the 'vascular' term revealed four
136 enriched pathways (Figure 3B), comprehending the regulation of vasculature and the adhesion of
137 leukocytes to vascular endothelium, which is a hallmark of inflammatory processes. However, the
138 investigation of the 'endothelium' term alone did not result in any significant enrichment.

139 **Genetic variation and gene expression across reference human brain samples depicts local
140 susceptibility to NTRK2**

141 Our current analyses have highlighted NTRK2 as a significant translational marker in all enriched
142 pathways for humans and mice (Fig 2 A and Fig 3 C). Next, the GTEx analysis revealed that the basal
143 ganglia, especially the putamen, exhibited the highest levels of NTRK2 expression, followed by the
144 frontal cerebral cortex (Figure 4A). Sex-biased expression in the included regions was tested for using
145 bulk gene expression. However, despite the putative higher expression observed in female donors, there
146 were no sex differences observed in the regions of the basal ganglia or the cerebral cortex (Figure 4B).

147 **DISCUSSION**

148 In this study, we assessed the involvement of the ChP in neuroinflammation during relapses in MS
149 patients through proteome profiling of human CSF on a molecular basis. We further conducted RNA
150 sequencing of ChP tissue in the EAE mouse model to mechanistically investigate the related patterns of
151 neuroinflammatory attacks and the similarities in humans and mice. We identified five highly enriched
152 proteins associated with ChP hypertrophy during relapses in both studied MS patient cohorts. Of the
153 five proteins examined, NTRK2 emerged as a reliable translational indicator of acute neuroinflammation
154 in both humans and mice. Our extensive translational analyses showed a significant involvement of
155 tyrosine kinase pathway signalling during the inflammatory phase in MS. This mechanism may
156 orchestrate cellular responses and tissue damage through cellular signalling and maintenance of the

157 inflammatory response. Two other proteins, ADAM23 and CPM, were related to cell adhesion through
158 interactions with integrins and other adhesion molecules as well as kinin-kallikrein system activation in
159 neuroinflammation.

160 In a recent study, we demonstrated that the enlargement of the ChP in MS aligns with
161 neuroinflammatory processes emphasizing its pivotal role in mediating interactions between the
162 peripheral and central immune systems (6). Together with the BBB, the blood CSF barrier (BCSFB) in
163 the ChP acts as a selective gatekeeper for immunoinflammatory response in the CNS. Despite these
164 insights, the biological mechanisms underlying volumetric alterations in the ChP in MS patients have
165 remained elusive.

166 Post mortem studies in MS patients have unveiled an accumulation of antigen-presenting cells in the
167 ChP stroma, disruption of tight junctions within the ChP epithelium, and an activation of immune cells
168 (5, 13). Under homeostatic conditions, the endothelium of the ChP is physiologically permeable (in
169 contrast to the BBB). Moreover, peripheral inflammatory processes like intestinal inflammation may
170 influence ChP permeability (1, 14). However, the molecular mechanisms underlying these dynamic ChP
171 abnormalities were not previously studied. Therefore, our study offers a first mechanistic perspective of
172 the processes pertaining to the ChP integrity, as measured with MRI and CSF dynamics during
173 inflammation.

174 To gain a better understanding of the pathophysiological mechanisms dependent on the ChP during an
175 inflammatory attack, we have dissected the biological and molecular pathways in which the observed
176 CSF proteins operate. The identified pathways encompassed cellular communication and signalling
177 (such as tyrosine kinase receptor activity and binding) as well as cell migration and plasticity induction
178 (including cellular generation, differentiation, and migration). Consistent with this, a recent study by
179 Elkjaer et al., (11) reported "cellular migration" as a major characteristic enriched in all MS subtypes,
180 including relapse, secondary progressive, and primary progressive MS. Our study depicts a more in-depth
181 view with the description of the transmembrane receptor protein tyrosine kinase activity followed
182 by the transmembrane signalling and vascular endothelial growth factor receptor activity as key
183 mechanisms in the molecular functional pathways analysis. The key pathways detected indicate the
184 involvement of inflammatory and vascular endothelial functions as key modifiers in ChP hypertrophy
185 for MS patients in relation to acute neuroinflammation. Another vital point is the detection of these
186 pathways in the conducted EAE mouse model. Recognizing the presence and relevance of these
187 pathways in an in vivo model that closely recapitulates human disease conditions enhances the
188 likelihood that our findings could be translated into meaningful therapeutic strategies for MS patients.

189 Regarding the central role of NTRK2, protein tyrosine kinases, which are the most important factors
190 found in our study, are key components of various signalling pathways that regulate immune cells,

191 including T and B lymphocytes. In MS, tyrosine kinases directly modulate the functions of B cells,
192 macrophages, and microglia therefore targeting both adaptive and innate mechanisms that contribute to
193 the immunopathology of MS on both sides of the BBB (15). Activated tyrosine kinases downstream of
194 immune cell receptors contribute to immune response promotion, inflammation, and tissue damage.
195 Given the critical involvement of tyrosine kinases in MS pathology, targeted therapies aimed at
196 modulating immune responses may help better mitigate the disease's impact on patients' quality of life.
197 An example of this is the treatment with CNS-penetrant BTK (Bruton tyrosine kinase) inhibitors. This
198 treatment option is currently under efficacy evaluation in clinical trials, but preclinical studies in the
199 EAE model have shown promising results in which key pathological features of MS, including B cell
200 activation, CNS lymphocyte infiltration, leptomeningeal inflammation, pro-inflammatory microglial
201 activation, and demyelination can be suppressed (16). See Kramer et al., (15) for a recent overview on
202 this topic.

203 Regarding specific attested proteins, the tyrosine kinase NTRK2 showed a robust correlation with ChP
204 volumes in both cohorts and was the highest enriched gene on both humans and mice. NTRK2 plays an
205 essential role in biological pathways including brain plasticity, impacting neuron survival, proliferation,
206 migration, differentiation, and synapse formation. All these pathways were indeed enriched in our study.
207 NTRK2 is a specific receptor of the Brain-Derived Neurotrophic Factor (BDNF). The binding results in
208 the activation of the MAPK pathway and regulation of synaptic plasticity and repair (17). Furthermore,
209 it can bind NTF4/neurotrophin-4 and NTF3/neurotrophin-3, which regulates neuron survival. A recent
210 genetic study, detected that the NTRK2 gene (of note, together with the STAT3 gene) has a significant
211 overlap in the genetic susceptibility of MS and linked psychiatric comorbidity (18). In their paper, the
212 NTRK2 gene had the highest enrichment and participated in the main signalling pathways (i.e. immune
213 interaction, cytokine responses) that were identified. In line with these findings, in our study, NTRK2
214 showed high PPIs and involvement in the enriched pathways in both cohorts. Overall, the involvement
215 of NTRK2 in the ChP of MS patients suggests its potential significance in regulating neuroinflammatory
216 processes, maintaining barrier integrity, and providing neurotrophic support.

217 The GTEx data revealed the highest expression of NTRK2 in the basal ganglia, particularly in the
218 putamen, of the human brain. The involvement of the putamen in MS has been established in untreated
219 patients with clinically isolated syndrome (CIS) (19) and in patients with different types of MS (19-21),
220 with increased vulnerability to lesion formation and demyelination (22).

221 The examined mouse model has highlighted immune-related and cellular communication pathways that
222 closely mirror the human results. This underscores the sensitivity of CSF measurements to detect
223 molecular abnormalities in ChP tissue. Additionally, the targeted search analyses reiterated a significant
224 involvement of tyrosine kinase metabolism and vascular components in neuroinflammation in both
225 humans and mice. Given, that the ChP integrity is associated with both inflammatory activity and

226 specific proteins, inhibition of the function of these molecules or their expression may influence disease
227 activity. Thus, our findings suggest the potential for ChP as a therapeutic target whilst highlighting its
228 mechanistic implications in neuroinflammation and neurodegeneration.

229 This study has limitations. The different MRI acquisition protocols in the two patient cohorts may
230 introduce variations in ChP segmentation. However, there were no significant differences in the
231 resulting volumes between both cohorts. Moreover, both groups of patients were recruited with the exact
232 same clinical inclusion criteria and protein sequencing, therefore, reducing the bias on clinical and
233 sampling acquisitions settings. Nonetheless, further validation in larger cohorts is essential to confirm
234 the detected non-inflammatory pathways and compensatory effects amid ChP characteristics.

235 Overall, our results provide new insights into the underlying mechanisms of acute neuroinflammation
236 in MS through non-invasive ChP characterisation, protein expressions in CSF, and the description of
237 the underlying mechanisms on a mesoscopic and molecular basis. Given the complexity and dynamic
238 pathogenesis of MS, our results highlight the possible future role of tyrosine kinase pathway modulation
239 targeting immune cell activation and migration. Depending on the specific targets, strong
240 immunomodulatory effects could potentially impact the inflammatory processes seen in MS. Overall,
241 our research offers novel prospects to thoroughly investigate multiscale networks and mechanisms
242 within the inflammatory CNS attacks, with a focus on the interplay between the peripheral and central
243 immune system. This could pave the way for innovative therapeutic interventions that might modify the
244 disease trajectory of MS.

245

246 MATERIAL AND METHODS

247 *Ethics statement*

248 The study was conducted in accordance with the Declaration of Helsinki and approved by the local
249 ethics committee (ethics committee of the Landesärztekammer Rhineland Palatinate, number
250 837.479.17 [discovery cohort] and number 837.019.10 [replication cohort]). Written informed consent
251 was obtained from all participants.

252 *Patient cohorts*

253 Patients form the discovery cohort belonged to larger MS cohort (n = 1156) with prospective
254 comprehensive and standardized clinical and standardized 3T MRI data collection from the Department
255 of Neurology at the University Centre Mainz. For the current analyses a group of 69 patients with
256 relapsing remitting multiple sclerosis (RRMS), confirmed according to the revised 2010 McDonald

257 diagnostic criteria, cursing a relapse period, and having CSF sampling for protein analyses were
258 included. The replication cohort consisted of patients from the outpatient clinic, which were diagnosed
259 using the same clinical criteria and but their MRI protocol was not standardized.

260 For the discovery cohort, individual images were acquired on 3T MRI scanner (Siemens Skyra) with a
261 3D T1 MPRAGE axial sequence with following parameters: Echo Time (ET) = 0.0025, Repetition Time
262 (RT) = 1.6, Inversion Time (IT) = 0.9, Flip Angle (FA) = 8°, matrix size = 200x256x192, voxel size =
263 0.9mm³. The second (replication) cohort (n=30) was included from the same department. For the
264 replication cohort, the scans were acquired on the same scanner using a modified 3D T1 MPRAGE
265 sagittal sequence with following parameters: ET = 0.0024, RT = 1.9, IT = 0.9, FA = 9°, matrix size =
266 192x256x256, voxel size = 1mm³. Each patient was clinically assessed by an experienced neurologist,
267 and the Expanded Disability Status Score (EDSS) score was determined at disease onset (study
268 entrance), annually for two years, and after four years. In total, MRI, clinical, and CSF proteomic data
269 from 99 RRMS patients were available and were included in the study.

270 ***Human MRI processing***

271 Magnetic resonance imaging preprocessing was performed using the open-source FreeSurfer
272 (<https://surfer.nmr.mgh.harvard.edu/>) software, which is currently the most widely used software to
273 automatically segment the brain structures, including the ChP. Details on the segmentation procedures
274 can be found elsewhere (23). In brief, FreeSurfer uses a probabilistic atlas built from manual
275 segmentations of a training dataset normalized to the MNI305 space. This allows a point-to-point
276 correspondence between all the training subjects. The atlas provides the probability of each label at each
277 voxel, the probability of each label given the classification of neighboring voxels (neighborhood
278 function), and the probability distribution function of voxel intensities, modelled as a normal
279 distribution, for each label at each voxel. The segmentation of a new individual MRI is achieved by
280 spatially registering the new subject to the MNI305 space and incorporating the subject-specific voxel
281 intensities to find the optimal segmentation that maximizes the probability of observing the input data.
282 FreeSurfer allows the segmentation of both the ChP and the CSF. Segmentation using FreeSurfer was
283 visually inspected and corrected where necessary for each subject.

284 ***Human protein analyses***

285 CSF sample collection was performed via lumbar puncture according to standard procedures (24, 25).
286 The CSF samples were then assayed using the proximity extension assay technology (PEA) (Olink
287 Proteomics AB, Uppsala, Sweden), in which 92 oligonucleotide-labelled antibody probe pairs
288 representing proteins related to the nervous system are allowed to bind to their respective target present
289 in the sample (Olink Target 96 Neurology panel). The PEA technique has a high specificity and

290 sensitivity (26). The platform provides Normalized Protein eXpression (NPX) data where a high protein
291 value corresponds to a high protein concentration, but not to an absolute quantification. NPX are
292 obtained by a series of computations. These operations are designed to minimize technical variation and
293 improve interpretability of the results. All assay validation data (detection limits, intra- and inter-assay
294 precision data, etc.) are available on the manufacturer's website (www.olink.com).

295 In order to investigate the biological activities that are regulated through the identified ChP associated
296 proteins, we explored protein–protein interactions (PPIs) using the STRING database (27), by using the
297 correlation values as ranks for the ontology and enrichment (28, 29). For functional annotation of the
298 significantly associating proteins, we effectuated Gene Ontology analysis within STRING. This allowed
299 for the identification of specific biological and molecular pathways to which these significantly different
300 proteins belong to.

301 To establish a link between the observed pathways and inherited brain susceptibility to disease, we
302 employed the Genotype-Tissue Expression (GTEx) portal (<https://gtexportal.org/home/>) by searching
303 the gene(s) that were commonly enriched in both humans and mice (see more details on mouse
304 experiments below). Correlations between genotype and tissue-specific gene expression levels help
305 identify regions of the genome that influence whether and how strongly a gene is expressed. GTEx helps
306 researchers to understand inherited susceptibility to disease. The dataset included 205 samples, of which
307 156 corresponded to male donors. This allowed for examining, using bulk gene expression, of sex-bias
308 in all available brain structures.

309 ***EAE mouse experiments***

310 EAE (experimental autoimmune encephalomyelitis) was induced in C57BL6J mice (N = 5; females, 9
311 weeks old at the start of treatment, Envigo) using a subcutaneous injection of 200mg of MOG peptide
312 (Myelin Oligodendrocyte Glycoprotein Peptide Fragment 35 to 55; from Charité) emulsified in
313 complete Freund's adjuvant (from Sigma-Aldrich) that contained 200mg of Mycobacterium tuberculosis
314 H37RA (from Difco). Pertussis toxin (400 ng; Enzo Life Sciences) was injected intraperitoneally in
315 200mL phosphate-buffered saline (PBS) on the day of immunisation and again two days later. Two
316 independent investigators scored disease severity daily in an anonymised manner using a 0 to 5 scale
317 (EAE score), as described elsewhere (30). The peak of demyelination occurs 10 to 15 days after
318 injection.

319 **RNA sequencing**

320 Choroid plexus (ChP) tissue was obtained for bulk RNA sequencing analyses from both naive and EAE
321 (day 14) samples. Using an established protocol (6, 31), ChP tissue was manually dissected from the
322 lateral, third, and fourth ventricles with the aid of an illuminated stereo microscope. The procedure
323 involved digestion of tissue from a single mouse in 300 µL of Hank's balanced salt solution (HBSS)

324 (Gibco; Catalogue number: 14025-092) containing collagenase and dispase (Merck; Catalogue number:
325 11097113001; concentration: 0.1 mg/mL) for 30 minutes at 37 °C using an orbital shaker. The
326 homogenised tissue was then passed through a 70-µm pore size cell strainer using an insulin syringe and
327 washed with 600 µL HBSS solution. Finally, the sample was centrifuged at 500 × g for 5 minutes at
328 room temperature. The supernatant was discarded, and the cellular pellet was suspended in 350 µL of
329 RLT buffer. RNA isolation was carried out by using a Qiagen RNeasy Micro Kit (Catalog No. 74004)
330 in accordance with the instructions provided by the manufacturer. The quality and quantity of RNA were
331 confirmed using NanoDrop and Bioanalyzer RNA 6,000 nano Kit (Agilent). Samples with RNA
332 integrity number values exceeding 6.5 were used for RNA sequencing. NEBNext ribosomal RNA
333 depletion was conducted, followed by NEBNext directional Ultra RNA II Library preparation and
334 sequencing on the NextSeq500 platform (Illumina) using the high output version 2 kit with 75 cycles.
335 To eliminate low-quality reads, fastp (32) was employed, and overrepresented sequences were analyzed.
336 In addition, polyG and polyX tail trimming was performed with parameters set to -g -x -p. The data
337 quality of the trimmed output was verified using fastqc. The data were aligned to the most recent
338 reference genome for mice (GRCm39) using the Spliced Transcript Alignment to a Reference aligner,
339 which is designed for long-reads. Samtools filtered out low-quality alignments, leaving only high-
340 quality alignments that were quantified using StringTie. The org.Hs.eg.db and org.Mm.eg.db databases
341 were used for annotation.

342 Next, we analysed the variance in gene expression between naive and EAE (14-day) mice via the
343 DESeq2 package on R-studio. This was followed by a protein-related gene search to assess protein-
344 interaction networks. Specifically, we utilized the Search Tool for the Retrieval of Interacting Genes
345 (STRING) database (<http://www.string-db.org/>) with a confidence score of 1 to form the foundation for
346 the functional study of the proteome. To examine the translational properties of the discovered networks
347 in the human proteome, we conducted a targeted search on the EAE data. To do so, we utilized PiNGO
348 (Version 1.5.2; <http://www.psb.ugent.be/esb/PiNGO>) in Cytoscape 3.9.1, a tool that identifies candidate
349 genes in biological networks that are predicted to be involved in specific processes or pathways of
350 interest. In summary, PiNGO permits a limited exploration of the ChP protein coding genes' engagement
351 in specific acknowledged roles via a straightforward network-based technique and Gene Ontology
352 categorization systems. PiNGO evaluates enrichment statistics using a hypergeometric test and regulates
353 the resulting P-values for several analyses using Benjamini-Hochberg FDR corrections (33). We
354 conducted the target search utilizing terms linked to 'tyrosine', 'vascular', and 'endothelium' pathways.

355 *Statistics*

356 Relevant proteins spectra were initially identified by spatially correlating NPX protein levels with ChP
357 volumes. Nuisance variables such as the total brain volume, age, and sex were used. Correction for
358 multiple comparisons was completed at a false discovery rate (FDR) of 5%, indicated by "pFDR". To

359 ensure the robustness of the associations, the same set of analyses was performed in the replication
360 cohort.

361

362 **References**

- 363 1. S. Carloni *et al.*, Identification of a choroid plexus vascular barrier closing during intestinal
364 inflammation. *Science* **374**, 439 (Oct 22, 2021).
- 365 2. S. Klistorner *et al.*, Choroid plexus volume in multiple sclerosis predicts expansion of chronic
366 lesions and brain atrophy. *Annals of clinical and translational neurology* **9**, 1528 (Oct, 2022).
- 367 3. J. Müller, S. Noteboom, C. Granziera, M. M. Schoonheim, Understanding the Role of the
368 Choroid Plexus in Multiple Sclerosis as an MRI Biomarker of Disease Activity. *Neurology* **100**,
369 405 (Feb 28, 2023).
- 370 4. B. Engelhardt, K. Wolburg-Buchholz, H. Wolburg, Involvement of the choroid plexus in central
371 nervous system inflammation. *Microsc. Res. Tech.* **52**, 112 (Jan 1, 2001).
- 372 5. M. Vercellino *et al.*, Involvement of the choroid plexus in multiple sclerosis autoimmune
373 inflammation: a neuropathological study. *J. Neuroimmunol.* **199**, 133 (Aug 13, 2008).
- 374 6. V. Fleischer *et al.*, Translational value of choroid plexus imaging for tracking
375 neuroinflammation in mice and humans. *Proceedings of the National Academy of Sciences of
376 the United States of America* **118**, (Sep 7, 2021).
- 377 7. J. Müller *et al.*, Choroid Plexus Volume in Multiple Sclerosis vs Neuromyelitis Optica Spectrum
378 Disorder: A Retrospective, Cross-sectional Analysis. *Neurology(R) neuroimmunology &
379 neuroinflammation* **9**, (May, 2022).
- 380 8. V. A. G. Ricigliano *et al.*, Choroid Plexus Enlargement in Inflammatory Multiple Sclerosis: 3.0-T
381 MRI and Translocator Protein PET Evaluation. *Radiology* **301**, 166 (Oct, 2021).
- 382 9. S. Engel *et al.*, Association of intrathecal pleocytosis and IgG synthesis with axonal damage in
383 early MS. *Neurology(R) neuroimmunology & neuroinflammation* **7**, (May 4, 2020).
- 384 10. F. Steffen *et al.*, Serum Neurofilament Identifies Patients With Multiple Sclerosis With Severe
385 Focal Axonal Damage in a 6-Year Longitudinal Cohort. *Neurology(R) neuroimmunology &
386 neuroinflammation* **10**, (Jan, 2023).
- 387 11. M. L. Elkjaer *et al.*, CSF proteome in multiple sclerosis subtypes related to brain lesion
388 transcriptomes. *Scientific reports* **11**, 4132 (Feb 18, 2021).
- 389 12. J. Huang *et al.*, Inflammation-related plasma and CSF biomarkers for multiple sclerosis.
390 *Proceedings of the National Academy of Sciences of the United States of America* **117**, 12952
391 (Jun 9, 2020).
- 392 13. E. H. Wilson, W. Weninger, C. A. Hunter, Trafficking of immune cells in the central nervous
393 system. *J. Clin. Invest.* **120**, 1368 (May, 2010).
- 394 14. B. Parodi, N. Kerlero de Rosbo, The Gut-Brain Axis in Multiple Sclerosis. Is Its Dysfunction a
395 Pathological Trigger or a Consequence of the Disease? *Frontiers in immunology* **12**, 718220
396 (2021).
- 397 15. J. Kramer, A. Bar-Or, T. J. Turner, H. Wiendl, Bruton tyrosine kinase inhibitors for multiple
398 sclerosis. *Nature reviews. Neurology* **19**, 289 (May, 2023).
- 399 16. E. Bame *et al.*, Next-generation Bruton's tyrosine kinase inhibitor BIIB091 selectively and
400 potently inhibits B cell and Fc receptor signaling and downstream functions in B cells and
401 myeloid cells. *Clinical & translational immunology* **10**, e1295 (2021).
- 402 17. A. Giordano *et al.*, BDNF Val66Met Polymorphism Is Associated With Motor Recovery After
403 Rehabilitation in Progressive Multiple Sclerosis Patients. *Frontiers in neurology* **13**, 790360
404 (2022).

405 18. A. Sepehrinezhad *et al.*, STAT3 and NTRK2 Genes Predicted by the Bioinformatics Approach
406 May Play Important Roles in the Pathogenesis of Multiple Sclerosis and Obsessive-Compulsive
407 Disorder. *J Pers Med* **12**, (Jun 26, 2022).

408 19. N. Bergsland *et al.*, Subcortical and cortical gray matter atrophy in a large sample of patients
409 with clinically isolated syndrome and early relapsing-remitting multiple sclerosis. *AJNR. American journal of neuroradiology* **33**, 1573 (Sep, 2012).

410 20. C. Jacobsen *et al.*, Brain atrophy and disability progression in multiple sclerosis patients: a 10-year follow-up study. *J. Neurol. Neurosurg. Psychiatry* **85**, 1109 (Oct, 2014).

411 21. J. Kramer *et al.*, Early and Degressive Putamen Atrophy in Multiple Sclerosis. *International journal of molecular sciences* **16**, 23195 (Sep 25, 2015).

412 22. L. Haider *et al.*, Multiple sclerosis deep grey matter: the relation between demyelination, neurodegeneration, inflammation and iron. *J. Neurol. Neurosurg. Psychiatry* **85**, 1386 (Dec, 2014).

413 23. B. Fischl *et al.*, Whole brain segmentation: automated labeling of neuroanatomical structures in the human brain. *Neuron* **33**, 341 (Jan 31, 2002).

414 24. G. D'Haens *et al.*, Effect of PF-00547659 on Central Nervous System Immune Surveillance and Circulating beta7+ T Cells in Crohn's Disease: Report of the TOSCA Study. *Journal of Crohn's & colitis* **12**, 188 (Jan 24, 2018).

415 25. O. Stuve *et al.*, Immune surveillance in multiple sclerosis patients treated with natalizumab. *Ann. Neurol.* **59**, 743 (May, 2006).

416 26. E. Assarsson *et al.*, Homogenous 96-plex PEA immunoassay exhibiting high sensitivity, specificity, and excellent scalability. *PLoS one* **9**, e95192 (2014).

417 27. D. Szklarczyk *et al.*, The STRING database in 2021: customizable protein-protein networks, and functional characterization of user-uploaded gene/measurement sets. *Nucleic Acids Res.* **49**, D605 (Jan 8, 2021).

418 28. D. Bartres-Faz *et al.*, Characterizing the Molecular Architecture of Cortical Regions Associated with High Educational Attainment in Older Individuals. *J. Neurosci.* **39**, 4566 (Jun 5, 2019).

419 29. M. J. Grothe *et al.*, Molecular properties underlying regional vulnerability to Alzheimer's disease pathology. *Brain* **141**, 2755 (Sep 1, 2018).

420 30. S. Bittner *et al.*, Endothelial TWIK-related potassium channel-1 (TREK1) regulates immune-cell trafficking into the CNS. *Nat. Med.* **19**, 1161 (Sep, 2013).

421 31. T. R. Menheniott, M. Charalambous, A. Ward, Derivation of primary choroid plexus epithelial cells from the mouse. *Methods in molecular biology* **633**, 207 (2010).

422 32. S. Chen, Y. Zhou, Y. Chen, J. Gu, fastp: an ultra-fast all-in-one FASTQ preprocessor. *Bioinformatics* **34**, i884 (Sep 1, 2018).

423 33. S. Maere, K. Heymans, M. Kuiper, BiNGO: a Cytoscape plugin to assess overrepresentation of gene ontology categories in biological networks. *Bioinformatics* **21**, 3448 (Aug 15, 2005).

424

425

426

427

428

429

430

431

432

433

434

435

436

437

438

439

440

441

442

443 **Acknowledgements**

444 The authors thank all the patients who participated in the study and Kathleen Claussen for proofreading
445 this manuscript.

446 **Funding**

447 This work was supported by:
448 German Research Foundation (Deutsche Forschungsgemeinschaft [DFG]; grant CRC-TR-128)
449 National MS Society USA grant RFA-220339314
450 DFG (Radiomics SPP 2177; grants GR 4590/3-1 and GO 3493/1-1)

451 **Author contributions**

452 Conceptualization: G.G-E., S.G., F.L.
453 Methodology: G.G-E., T.R., J.G., P.S.W.
454 Investigation: G.G-E., J.S., F.L., S.G.
455 Visualization: G.G-E.
456 Funding acquisition: S.G., G.G-E., F.Z., O.S., F.L., V.F.
457 Project administration: F.L., V.F., J.S., P.S.W., J.G., T.B., S.G.M.
458 Supervision: S.G., F.L.
459 Writing – original draft: G.G-E., J.S., F.L.
460 Writing – review & editing: F.L., J.S., G-G-E., V.F., S.E., D.C., T.K., P.S.W., J.G., T.B., A.O., S.B.,
461 S.G.M., F.Z., O.S., S.G.

462 **Competing interests**

463 FL received consultancy fees from Roche and support with travel cost from Teva Pharma.

464 OS serves on the editorial boards of Therapeutic Advances in Neurological Disorders, has served on
465 data monitoring committees for Genentech-Roche, Pfizer, Novartis, and TG Therapeutics without
466 monetary compensation, has advised EMD Serono, Novartis, and VYNE, receives grant support from
467 EMD Serono, is a 2021 recipient of a Grant for Multiple Sclerosis Innovation (GMSI), Merck KGaA,
468 is funded by a Merit Review grant (federal award document number (FAIN) BX005664-01 from the
469 United States (U.S.) Department of Veterans Affairs, Biomedical Laboratory Research and
470 Development, and is funded by RFA-2203-39314 (PI) and RFA-2203-39305 (co-PI) grants from the
471 National Multiple Sclerosis Society (NMSS).

472 PSW reports outside the submitted work, consulting fees from Astra Zeneca, research funding from
473 Bayer AG, research funding, consulting and lecturing fees from Bayer Health Care, lecturing fees from

474 Bristol Myers Squibb, research funding and consulting fees from Boehringer Ingelheim, research
475 funding and consulting fees from Daiichi Sankyo Europe, consulting fees and non-financial support
476 from Diasorin, non-financial research support from I.E.M., research funding and consulting fees from
477 Novartis Pharma, lecturing fees from Pfizer Pharma, non-financial grants from Philips Medical Systems,
478 research funding and consulting fees from Sanofi-Aventis. He is principal investigator of the future
479 cluster “curATime” (BMBF 03ZU1202AA, 03ZU1202CD, 03ZU1202DB, 03ZU1202JC,
480 03ZU1202KB, 03ZU1202LB, 03ZU1202MB, and 03ZU1202OA) and principal investigator of the
481 DIASyM research core (BMBF 161L0217A), and principal investigators of the DZHK (German Center
482 for Cardiovascular Research), Partner Site Rhine-Main, Mainz, Germany.

483 The other authors declare no conflicts of interest related to this work.

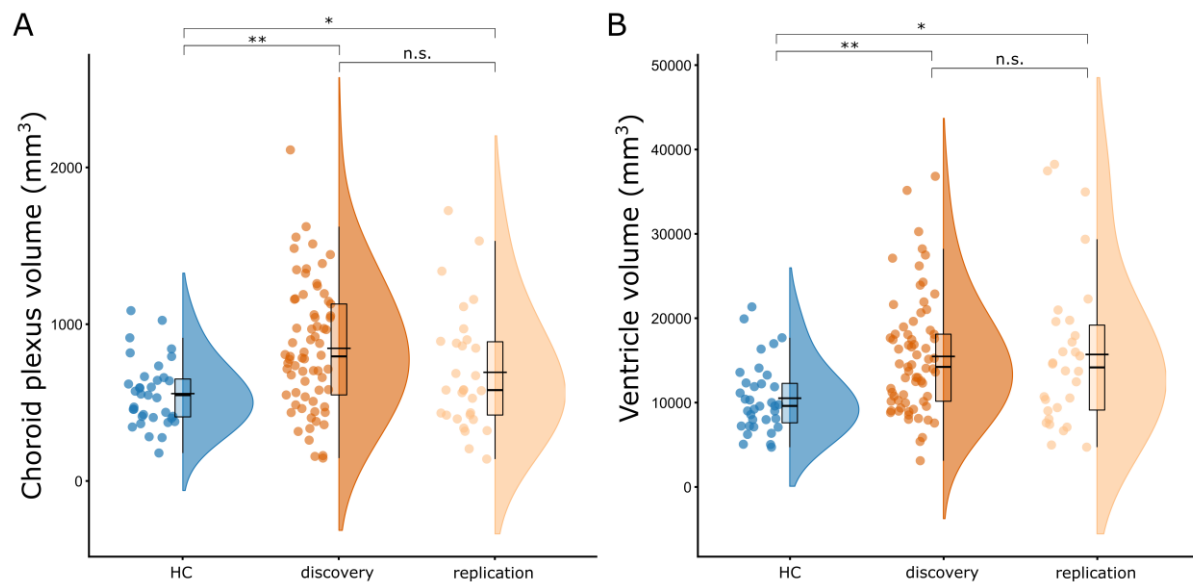
484 **Data and materials availability**

485 All the current work was performed using openly available software:
486 <https://surfer.nmr.mgh.harvard.edu/>, <http://www.string-db.org/>, <http://www.psb.ugent.be/esb/PiNGO>,
487 <https://gtexportal.org/home/>. Data cannot be made openly available due to institutional restrictions, but
488 it can be made available from the corresponding authors upon reasonable request and the corresponding
489 data transfer agreement (DTA).

490

491 **FIGURES**

492



493

494 **Fig. 1.** Comparison of ChP volumes between the healthy controls (HC; blue), discovery (orange) and
495 replication cohorts (light orange; left panel) and ventricle volume between the HC (blue), discovery
496 (orange) and replication cohorts (light orange). Age, sex and total brain volume (TBV) were used as
497 covariates in the model. *p<0.05, **p<0.001, n.s. (not significant).

498

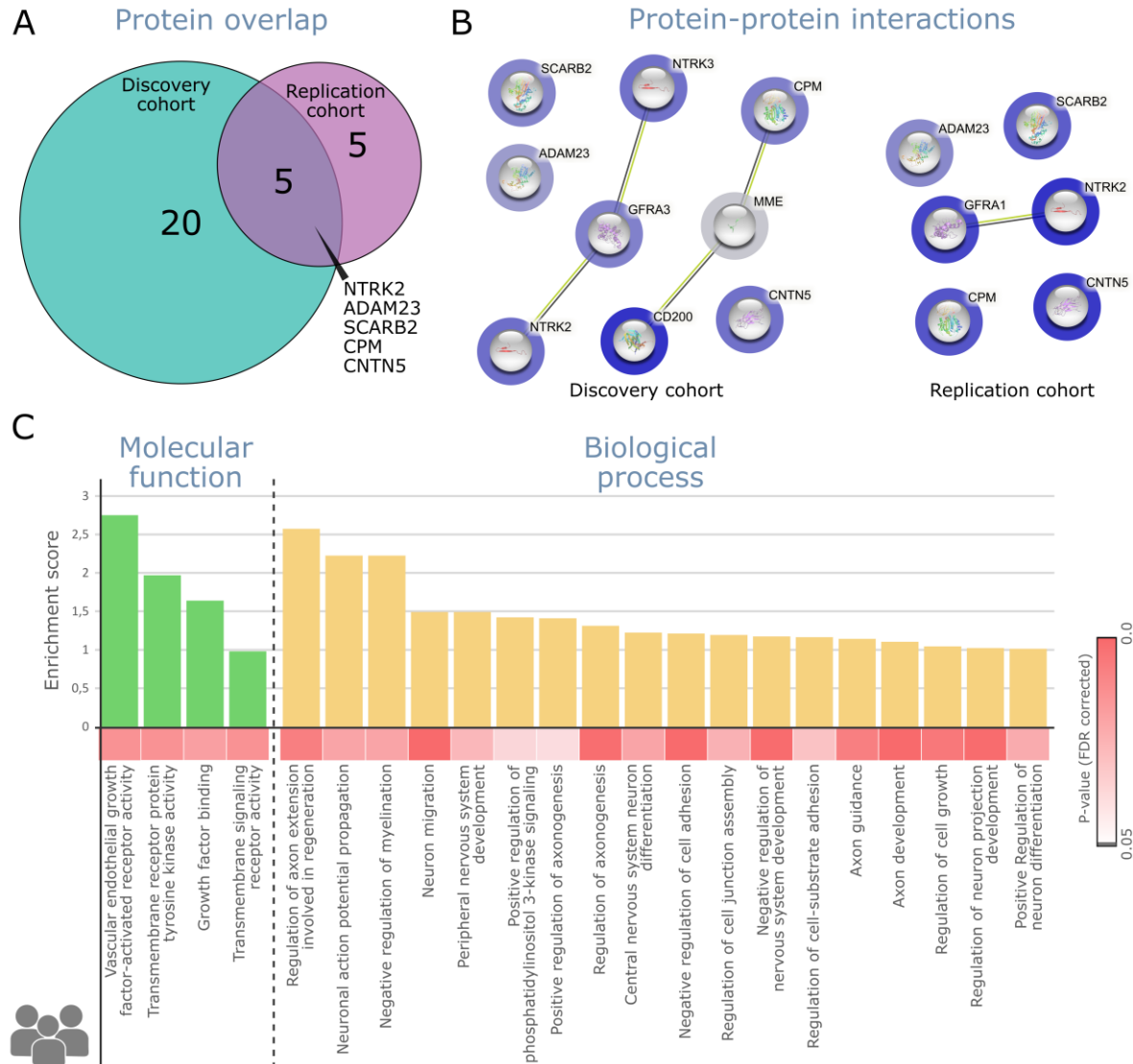


Fig. 2. Protein–protein interactions and functional annotation analyses. A) Venn diagram illustrating the proteins associating with the choroid plexus volume in both, the discovery (green) and replication (light purple) cohorts, as well as the overlapping proteins. B) Protein-Protein interaction (PPI) network for both the discovery (left) and the replication (right) cohorts. The blue scale colours on the circles indicate how strongly represented the proteins are in each sample, where darker colors indicate highly represented proteins. C) Downstream analyses. Significant enrichment for molecular function (green) and biological process (yellow) pathways.

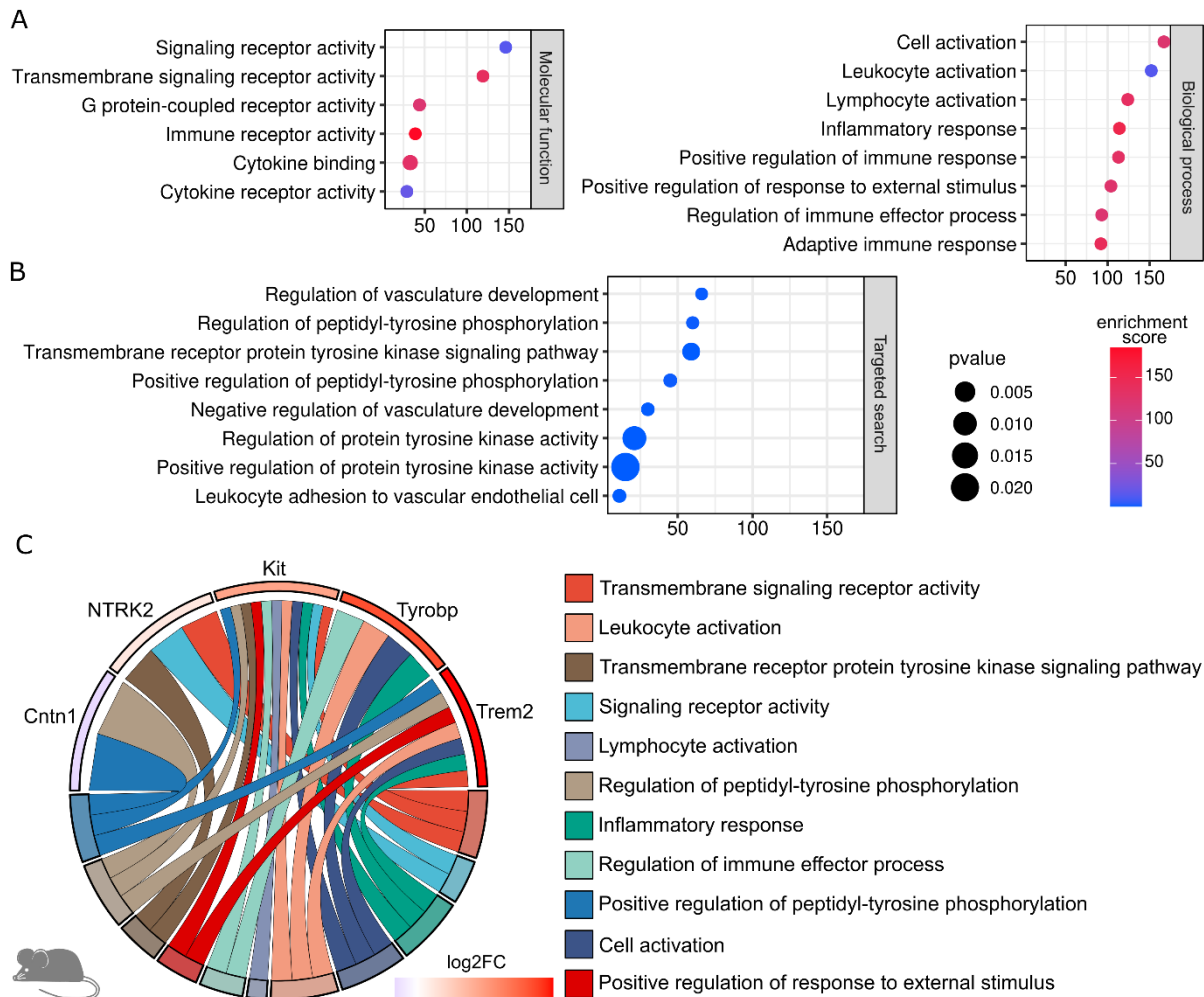
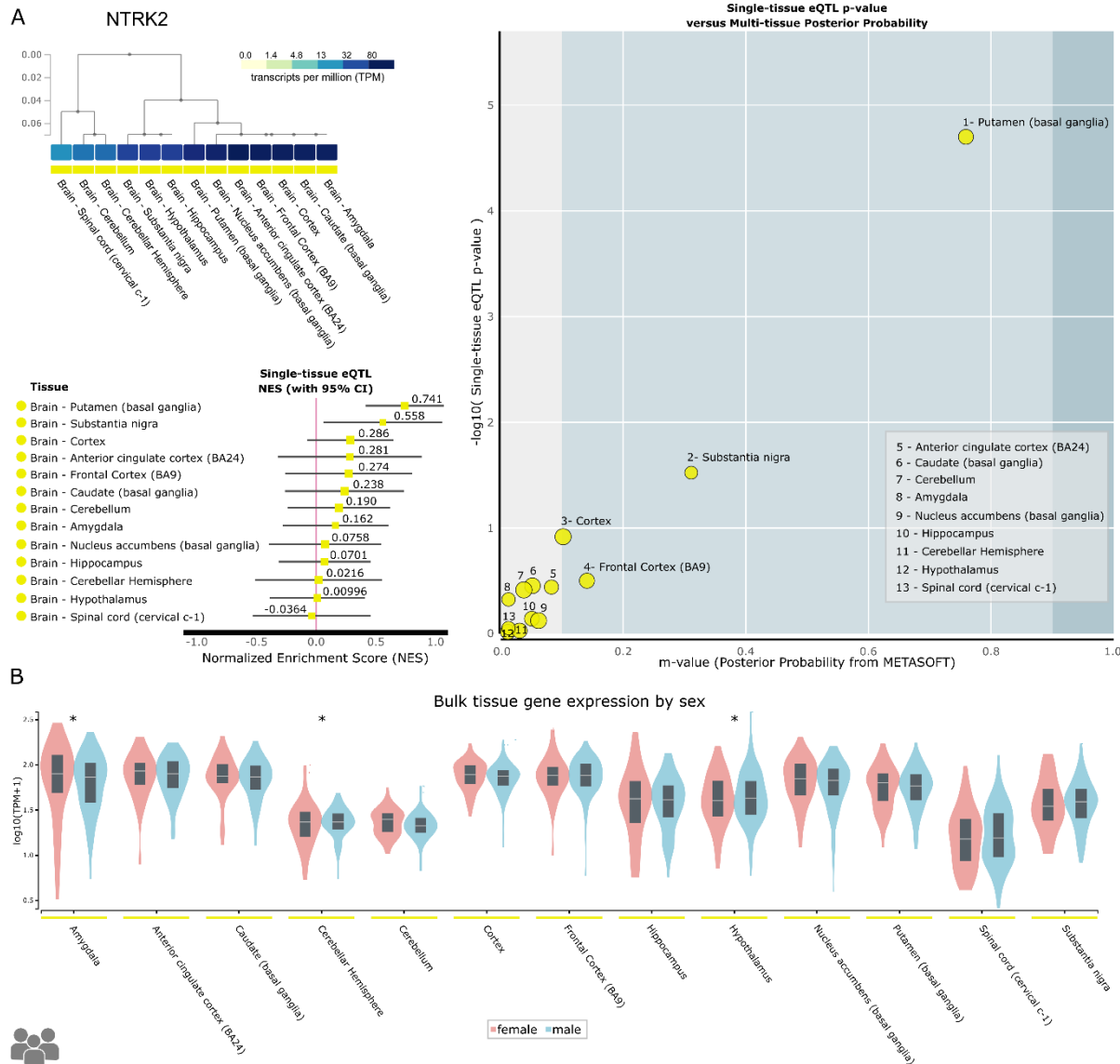


Fig. 3. Protein-interaction analyses in the mice model of inflammation. For these analyses, experimental autoimmune encephalomyelitis (EAE) mice were compared at the peak of inflammation (14 days) against baseline expression. The resulting fold2log change was used to create a Protein-Protein interaction (PPI) network depicting pathways that are differentially expressed during neuroinflammation. The downstream analyses evidenced significant enrichment of pathways similar to those in the human cerebrospinal fluid (CSF) samples (A). Additionally, the targeted analyses depicted further tyrosine kinase enriched pathways (B). C) The pathway chord diagram depicted that genes from the tyrosine protein kinase family (Cntn1, NTRK2, Kit, and Tyrobp) as well as tyrosine receptors (Trem2) were the most abundant among enriched pathways. In A and B, X-axis reflects the gene counts.



518

519 **Fig. 4. Results of the GTEx analysis for NTRK2.** A) Regional susceptibility analyses showing the
520 basal ganglia (putamen) and cortex (frontal area) as the regions with the highest expression of NTRK2
521 gene. B) Bulk gene expression for all regions depicted no sex-bias in the expression of NTRK2 gene
522 across the basal ganglia or cortical regions. Asterisks depict significant differences between male and
523 female.

524

525 **Table 1.** Clinical data of the discovery cohort and replication cohort

Clinical data	HC (n = 35)	Discovery cohort (n=69)	Replication cohort (n= 30)	Test statistic	P-value
Sex (female[%])	23 [64]	38 [55]	22 [73]	2.4*	0.12
Mean age \pm SD years	30.2 \pm 9	31.8 \pm 8.5	32.4 \pm 9.2	0.75†	0.48
Median EDSS \pm SD		2 \pm 0.8	2 \pm 1.1	2.24†	0.03
Disease duration in months as mean (range)		0 (0-4)	0 (0-3)	1.3†	0.21

*group comparisons performed using a χ^2 test

† group comparisons performed using ANOVA

HC = healthy controls; SD = standard deviation; EDSS = Expanded Disability Status Scale.

526 **Table 2.** Proteins associated with choroid plexus volume in the discovery and replication cohorts

	Discovery cohort		Replication cohort	
	r	P*	r	P*
NTRK2	0.382	0.013	0.44	0.048
ADAM23	0.37	0.019	0.445	0.045
SCARB2	0.356	0.028	0.392	0.05
CPM	0.334	0.027	0.4	0.044
CNTN5	0.327	0.033	0.451	0.041

*Presented P-values are corrected for multiple comparisons using FDR. r = r-score.

527

528